About modeling rheology and agglomeration of wet particle systems

Stefan Luding

Abstract:
This brief article is a review of our recent results on the flow-behavior and rheology of dry and wet cohesive particles. For weak and moderate strength of attractive forces, a new set of rheological laws was derived from particle simulations. This local granular rheology is based on the $\mu(I)$ and $\phi(I)$ rheology, generalized by multiplicative correction terms that depend on the inertial number I and on other dimensionless variables (like confining stress P^*, or the cohesive strength, as quantified by the local Bond number Bo) that characterize the local situation, the state the particles are in. Each correction relates to one (or more) mechanisms that are active in the powder – and the correction terms fall back to unity, i.e., become inactive, when a mechanism is not important, not relevant. Only if attractive forces are strong enough, when the local Bond number Bo>1, agglomeration kicks in and the rheology that is based on homogeneous flow situations becomes questionable.

1 Introduction

The behavior of particulate systems or granular matter – for example sand, powders, suspended particles as colloids or macro-molecules – is of interest for a wide range of industries and research disciplines. These materials are intrinsically disordered, come with a wide distribution of particle sizes and materials/mixtures and can behave both solid- or fluid-like, dependent on the balance between energy input (external parameters: agitation, driving) and energy dissipation (e.g., due to material properties: contact deformation, friction, viscosity). The micro-mechanical processes in particle systems are active at multiple scales (from nanometers to meters) and understanding them better is an essential challenge for both science and application, i.e., finding the reasons for natural/industrial disasters like avalanches or silo-collapse.

To understand the fundamental micro-mechanics one can use particle simulation methods. However, large-scale applications (due to their enormous particle numbers) must be addressed by upscaled coarse grains or by continuum theory. To bridge the gap between the discrete and continuum scales, so-called micro-macro transition methods translate particle positions, velocities, and forces into density-, stress-, and strain-fields. These macroscopic quantities must be compatible with the conservation equations for mass, momentum, and energy of continuum theory. Possibly, non-classical fields are needed to describe the micro-structure or the statistical fluctuations, e.g. the kinetic stress, before one can solve real application problems.

2 Granular state space

The particles are in different states: in different applications, in different systems, they are locally experiencing different situations. State variables are the shear or deformation rate, as quantified by the inertial number I (as relating the pressure- to the rate-time-scale) or the confining stress, as quantified by the dimensionless pressure P^* (as relating the contact-stiffness- to the pressure-time-scale, both squared). State variables can be interdependent, e.g., the inertial number depends inversely on the square-root of pressure.
On the other hand, the cohesive strength, strictly speaking, is a material parameter, as quantified by the gravity Bond number Bo_g that relates the cohesive forces to the gravity force on a single particle. However, the more relevant comparison is between the cohesive force and the local confining forces $f \propto Pd^2$, as quantified by the local Bond number Bo, which also renders it a state variable. See publications by Shi et al. (2020) and Roy et al. (2017) for the detailed definitions and rheology results from simulations, and Fig.1 for the state space spanned by I and P^*.

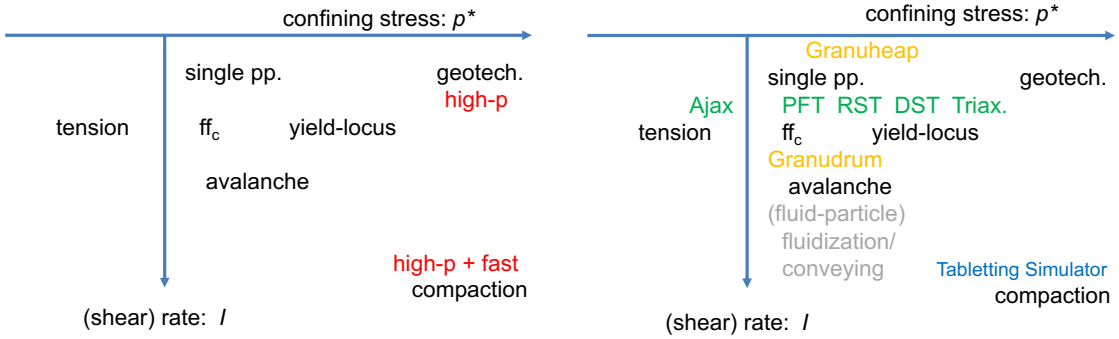

Figure 1: Schematic diagram of granular states in the plane of confining stress (to the right), tension (to the left) and dimensionless shear or deformation rate (vertical down); the left panel shows the state variables at their respective relevant location in state-space, while the right panel also indicates a selection of experiments that can be used at that states. [The experimental abbreviations are: Ajax Tensile Tester, PFT=particle flow tester, RST=ring shear tester, DST=direct shear tester, Triax=triaxial geotechnical tester, and the Granu* abbreviates GRANUTOOLS devices like heap-test or rotating drum.]

Evidently, most experiments can operate only in a limited domain in parameter space. Therefore, the tensile regime was combined with results from the RST device by Garcia-Trinanes et al. (2019) and the drum was connected to heap and RST situations by Shi et al. (2020b). The role of cohesion at various states/situations was studied by Roy et al. (2017); Shi et al. (2020) numerically, and by Jarray et al. (2019) experimentally – see also references therein.

2.1 Bridging between compression and tension

Powders with cohesive forces allow to range from compressive shear to tensile testing (Garcia-Trinanes et al. 2019). Measurement and prediction of cohesive powder behaviour related to aspects/phenomena such as flowability, flooding or arching in silos is challenging. Previous

attempts in comparing different testers did not yield reliable data (showing considerable scatter and uncertainty in key quantities). Studies to build a reliable experimental database using reference materials are needed to evaluate the repeatability and effectiveness of shear testers and the adopted procedures.

Shi et al. (2018) studied the effect of particle size on the yield locus for different grades of limestone (calcium carbonate). We use the non-linear Warren Spring relation for shear stress: $\tau(\sigma)/C=(\sigma/T+1)^{1/n}$, with confining stress σ, to obtain the values of cohesion C, tensile strength T, and the shear index n. We recover linear ($n = 1$) yield loci for large, free flowing particles, with respectively small C and T, with consistent, finite macroscopic friction $C/T = 0.7$. For particle size decreasing below 70 μm the response becomes more and more cohesive (larger C and T) and non-linear ($1<n<2$) – see Garcia-Trinanes et al. 2019; the latter $n>1$ implies that a linear fit ($n=1$) to the yield locus of a cohesive powder is not making much sense.

Then Garcia-Trinanes et al. (2019) compare the values of the parameters C, T and n obtained from two different shear testers (Schulze and Brookfield PFT). Both testers run at positive confining stresses (slightly different ranges and principles) and give identical results for large fractions (weakly cohesive). For strongly cohesive samples, the PFT results are very similar to the ring shear tester, with slightly smaller values for C, T, and n.

Finally, the (non-linearly extrapolated) values of T were compared with a direct, transverse measurement running at negative stresses, using the Ajax tensile tester, and very good agreement was found – validating the Warren Spring equation for negative stresses (Garcia-Trinanes et al. 2019). Further experiments with a variety of cohesive powders are needed to confirm the connection between moderate compression and tension, and also to confirm (or rebut) this systematic, consistent differences between shear testers for, so far, only one cohesive powder.

2.2 Bridging between low and high stress, slow and fast deformations

Because the flow behavior of powders depends on both their flow/deformation rate and confining stresses, as well as on their cohesive strength, it is difficult to measure/quantify powders with only one experiment. Commonly used characterization tests, which cover a wide range of states, were compared by Lumay et al. (2019): including (static, free surface) angle of repose, (quasi-static, confined) ring shear steady state angle of internal friction, and (dynamic, free surface) rotating drum flow angle/slope, using free flowing, moderately and strongly cohesive limestone powders.

Free flowing powder gives good agreement of the measured angles (slopes or shear resistance) among all different situations (devices), while the cohesive powders are more interesting. Starting from the flow angle in a rotating drum and going slower, one can extrapolate to the limit of zero rotation rate. However, the angle of repose measured from the static heap is considerably larger, possibly due to its special history. When the ring shear tester explores its lowest confining stress limit, the steady state angle of internal friction of the cohesive powder becomes comparable with the flow angle (at the free surface) in the zero-rotation rate limit of the rotating drum test, but only when defining an appropriate effective stress for the flow zone. Finally, when stretching the confining stress to extremely large values (GPa) by using a tableting tester, the qualitative behavior (increase of shear resistance, macroscopic friction with decrease in particle size) is confirmed, but the almost linear behavior in the low stress range (kPa to MPa) turns to an increasingly non-linear growth – details see Lumay et al. (2019) and Shi et al. (2018).

Also here, further experiments with a variety of cohesive powders are needed to confirm the connection between moderate to large compression/confining stress, and tension, and also to confirm the systematic, consistent qualitative trends, so far reported for one cohesive powder.

3 Granular rheology

Here, a short summary of recent results on formulating a general local granular rheology is presented, based on an earlier review by Luding et al. (2016). When formulating a granular rheology, the starting point is the successful, simple, and elegant so-called $\mu(I)$-rheology (Shi et al. 2020), which relates the so-called macroscopic (bulk) friction, i.e., the shear-stress to pressure ratio $\mu = \tau / p$ (in a sheared particulate system in steady state) to the inertial number, i.e., the dimensionless strain-rate:

$$I = \dot{\gamma} d_0 \Big/ \sqrt{p'/\rho}$$

with (for example) local shear rate $\dot{\gamma}$, diameter d_0 = 0.0022 m, mass-density ρ= 2000 kg/m^3, and pressure p'. The relation that describes well a wide variety of flows of hard, cohesionless particles, at various strain rates is:

$$\mu(I) = \mu_0 + (\mu_\infty - \mu_0)\,\frac{1}{1 + I_0/I} \tag{1}$$

with $\mu_0 = 0.15$, $\mu_\infty = 0.42$, and $I_0 = 0.06$, matching our simulation data (Roy et al. 2017), where μ_0 and μ_∞ represent the zero and infinite strain rate limits, respectively, and the characteristic dimensionless strain-rate is I_0, above which inertia effects considerably kick in. Since our older simulations (Roy et al. 2017) concern particle simulations with a very small coefficient of particle contact friction, μ_p = 0.01, the dependence of the coefficients in Eq. (1) on friction is not considered, however, Shi et al. (2020) extended and generalized the rheology for a wide range of coefficients of friction.

The first correction to the $\mu(I)$-rheology is relevant for soft particles, as based on early results; it was originally given as linear additive term to the above rheology for small strain-rates, however, it can nicely be re-phrased as multiplicative correction factor:

$$\mu(I,p) = \mu(I)\left(1 - \left(\frac{p}{p_0}\right)^{1/2}\right) f_\mu(\mathrm{Bo}) \tag{2}$$

with the dimensionless pressure $p = p'\, d_0 / k$, the characteristic pressure at which this correction becomes considerable, p_0 = 0.9, and the stiffness k = 100 N/m. This correction accounts for a range of particle stiffness (or softness), but also for different magnitudes of gravity, as one would find in a centrifuge or on the moon. Describing granular flows using such a local approach, in opposition to non-local models, saves the beautiful simplicity of locality and nevertheless extends the basic model by including neglected features. Additional corrections f_μ(Bo) for cohesive particles involve non-linear functions of the Bond-number (see Roy et al. 2017; Shi et al. 2020; and references therein), but are omitted in the following.

Both dimensionless state variables can be expressed as a ratios of time-scales, namely $I = t_\gamma / t_p$ and $p = \left(t_p / t_c\right)^2$, where the subscripts denote strain-rate-, pressure- and contact-stiffness-time-scales, respectively. To complete the rheology for soft, compressible particles, a relation for the density as function of pressure and shear rate is missing:

$$\phi(I,p) = \phi_c \left(1 + \frac{p}{p^c_\phi}\right)\left(1 - \frac{I}{I^c_\phi}\right) g_\phi(\mathrm{Bo}) \qquad (3)$$

with the critical or steady state density under shear, in the limit of vanishing pressure and inertial number $\phi_c = 0.648$, the strain rate for which dilation would turn to fluidization $I^c{}_\phi = 0.85$, and the typical pressure level for which softness leads to huge densities $p^c{}_\phi = 0.33$ (Luding et al. 2016). Both correction terms could be more complex functions, but are presented in their first order linear term only, valid only for sufficiently small arguments: Too large inertial numbers would fully fluidize the system so that the rheology should be that of a granular fluid, for which kinetic theory applies, while too large pressure would lead to enormous overlaps, for which the contact model and the particle simulation become questionable. The considered inertial numbers are $I < 0.1$, while the pressures are $p < 0.01$. Additional corrections $g_\mu(\mathrm{Bo})$ for cohesive particles (Shi et al. 2020) are omitted in the following.

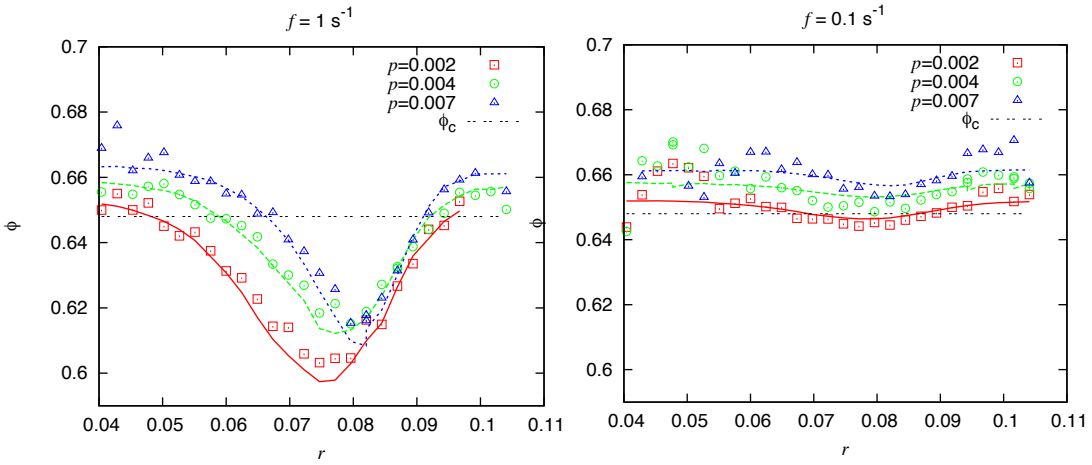

Figure 2: Density for rapid (left) and moderate (right) rotation frequency, plotted against the radial distance r, with data from particle simulations (from Luding et al. 2016), using the external rotation frequency f, given above the panels, filtered at three different (approx.) pressure levels, p, as given in the inset (i.e. red, green and blue correspond to: close to the surface, in the middle, and closer to the bottom). The lines correspond to Eq. (3), with all parameter values given in the main text; the horizontal lines give the low stress and strain-rate limit ϕ_c that, notably, is not the asymptotic limit.

From a rapid and moderate external rotation frequency, f, of the split-bottom ring shear cell, with split at R_s = 0.085 m, representative data from Roy et al. (2017), are plotted in Fig. 2 against the radial position. Higher confining stress corresponds to a higher density, deeper below the free surface, while the density is reduced in the shear band, proportional to the local shear-rate, due to dilatancy. Overall, the simulation data agree very well with the corrected density prediction from the analytical Eq. (3), where only local information enters, besides some scatter and more systematic deviations in the tails of the shear band, away from the split, with very small local strain rates (the statistics is poor, and the system is not yet in steady state).

The macroscopic friction, i.e., the shear stress ratio μ, is plotted in Fig. 3, against the radial position for the same data-sets, in comparison with the classical rheology of Eq. (1) and the pressure-dependent rheology, Eq. (2). The pressure dependence is improved when using the latter, especially in the tails, for the slower rotation rate, where the classical rheology has no pressure dependence. Nevertheless, in the tails the stress ratio does not agree well with theory, indicating missing additional correction terms that account for a combination of very low strain-rate and finite granular temperature effects, playing a role in those regimes.

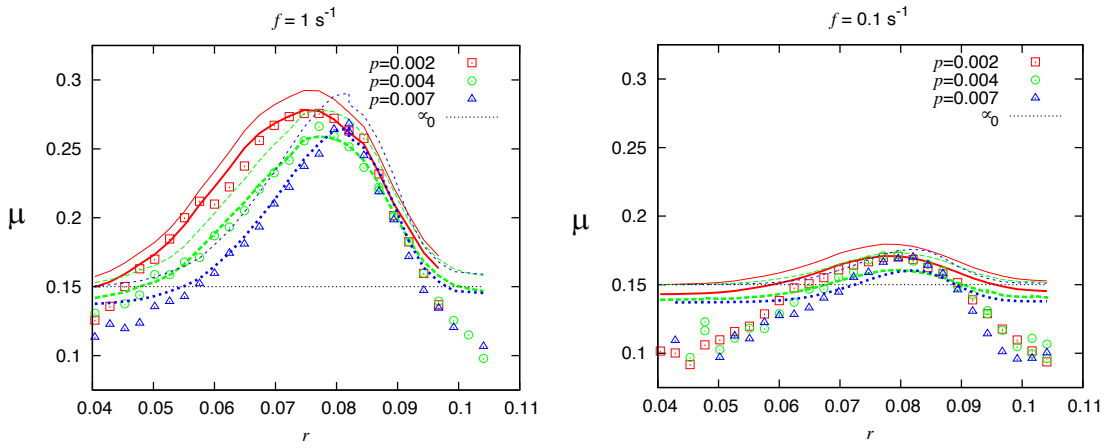

Figure 3: Shear stress ratio μ, for the same simulations as in Fig. 2 (from Luding et al. 2016). Lines correspond to Eq. (1), classical rheology (thin lines), or Eq. (2), corrected soft rheology (thick lines); parameters are given in main text. The horizontal dotted lines give the constant low strain-rate limit, μ_0.

4 Conclusion and Outlook

In conclusion, particle simulations can complement experiments, and the micro-macro transition can guide the development of new rheological particle-flow or continuum scale rheology models for density and shear stress ratio. The presented rheology includes and combines various mechanisms, as quantified by characteristic dimensionless numbers – for various different material properties including contact friction and attractive forces (Shi et al. 2020). The original, simple, scalar $\mu(I)$ and $\phi(I)$ rheology for flowing rigid, cohesionless particles was generalized to take into account the effects of large confining stress and/or softness (compressibility) of the particles, as well as attractive contact forces (Roy et al. 2017; Shi et al. 2020). Both the local density and shear stress to pressure ratio are well predicted by an improved, pressure dependent local rheology model, especially in the centre of the shear band – not so much in the tails, where the mechanism of creep becomes relevant for the shear resistance and needs to be included, as proposed by Roy et al. (2017). The deviations that still occur in the tails can be due to several reasons: (i) the statistics is much worse in areas where the strain rate is small, (ii) the system has not yet reached the true steady state – as reported previously (see Roy et al. 2017 and references therein), (iii) there can be non-local effects as encompassed, e.g., by a "fluidity" or granular temperature variable, (iv) there can be a missing parameter that encompasses the micro-structure, or further additional local corrections are needed, not considered so far. Ongoing research is aiming at finding such further corrections for very small strain rates, but also for cohesive particles. As next step the implementation of

novel multi-purpose, generalized flow/rheology models into continuum solvers is needed. A further goal is the development of fully tensorial flow models, to account for all the non-Newtonian aspects of particulate and granular matter, for both static and dynamic situations and transients as well.

References

[1] Shi, H., Roy, S., Weinhart, T., Magnanimo, V. Luding, S. (2020): Steady state rheology of homogeneous & inhomogeneous cohesive granular materials, *Granular Matter* 22, 14

[2] Roy, S., Luding, S., Weinhart, T. (2017): A general(ized) local rheology for wet granular materials, *New J. Phys*. 19, 043014

[3] Shi, H., Lumay, G., Luding, S. (2020b): Stretching the limits of dynamic and quasi-static flow testing on cohesive limestone powders, *Powder Technology* 367, 183-191

[4] Garcia-Trinanes, P., Luding, S., Shi, H. (2019): Tensile strength of cohesive powders, *Advanced Powder Technology* 30(12), 2868-2880

[5] Jarray, A., Shi, H., Scheper, B. J., Habibi, M., Luding S. (2019): Cohesion-driven mixing and segregation of dry granular media, *Scientific Reports* 9(12), 13480

[6] Shi, H., Mohanty, R., Chakravarty, S., Cabiscol, R., Morgeneyer, M., Zetzener, H., Ooi, J. Y., Kwade, A., Luding, S., Magnanimo, V. (2018): Effect of Particle Size and Cohesion on Powder Yielding and Flow, *KONA* 2018014, 226-250

[7] Luding, S., Singh, A. Roy, S. Vescovi, D., Weinhart, T., Magnanimo, V. (2016): From particles in steady state shear bands via micro-macro to macroscopic rheology laws, in: *Proceedings of the 7th International Conference on the Discrete Element Method*, Xikui Li, Yuntian Feng, Graham Mustoe (Eds.), ISBN: 978-981-10-1925-8 (Print) 978-981-10-1926-5 (Online)

Author

Stefan Luding, Prof. Dr. rer.-nat. Multi Scale Mechanics
Department Thermal and Fluids Engineering, Faculty of Engineering Technology
Universiteit Twente (UT), P.O. Box 217, 7500 AE Enschede, NL
Phone: +31-(0)53 489-4212, Secr.: -3371
e-mail: s.luding@utwente.nl,
web-site: https://www2.msm.ctw.utwente.nl/sluding/